PERGAMON

Journal of Structural Geology 22 (2000) 851–863

JOURNAL OF STRUCTURAL GEOLOGY

www.elsevier.nl/locate/jstrugeo

Possible absence of small faults in the Gullfaks Field, northern North Sea: implications for downscaling of faults in some porous sandstones

Haakon Fossen[a,*], Jonny Hesthammer[b]

[a]*Department of Geology, University of Bergen, Allegt. 41, N-5007 Bergen, Norway*
[b]*Statoil, N-5020 Bergen, Norway*

Received 19 April 1999; accepted 19 January 2000

Abstract

Faults and fractures have been studied in more than 6 km of cores from the Gullfaks Field, northern North Sea, and compared to fault populations determined by stratigraphic correlation of well logs and seismic data. Statistical analysis indicates a power-law correlation between displacement and fault frequency for displacements down to 5–10 m. Observations of deformation bands, with displacements ranging from 1 mm to 10 cm, perfectly fit the low-end extension of this power-law model. However, integrated use of well-log correlation data and core data indicates that few faults exist with displacement between ~20 cm and 5 m. If this data gap is real and representative for other sandstones, uncritical downscaling of seismic-scale fault sizes for use in oil reservoir description or strain estimation may yield erroneous results. The possible gap may be related to the high density and coalescent nature of (larger) faults, excluding the tip portions of many faults and thus the likelihood for wells to intersect low-displacement tip regions. Deformation bands, on the other hand, seldom develop displacements much in excess of ~10 cm, thus providing a distinct population of displacement data in the lower end of the displacement scale which, by coincidence, falls close to the extrapolated trend of the well data in log–log space.

1. Introduction

Much recent research on fault populations has focused on scaling laws or the distribution of faults of different lengths and displacements within volumes of fractured rocks. For purposes of calculating strain and, in particular, estimating properties and behavior of oil field reservoirs, knowledge of fault size distributions may be crucial (King and Cisternas, 1991; Walsh et al., 1991; Marrett and Allmendinger, 1992; Roberts et al., 1993; Gauthier and Lake, 1993). Such information is commonly sought for occasions where the main source of information is seismic data with or without additional core information from wells. Typical fault sizes include displacement, as discussed in the present article, length, height and fault zone thickness. The displacement–frequency distribution can in many cases be described by a power-law relationship, revealed by a straight data segment in cumulative log–log diagrams (e.g. Yielding et al., 1992; Jackson and Sanderson, 1993; Wojtal, 1994). Hence, denoting the displacement (or some other measure of fault size) by S, the number N of faults having a displacement greater than or equal to S is given by:

$$N = aS^{-D}.$$

The variable a is a constant and the exponent D is often referred to as the fractal dimension. Having established the scaling law, the frequency of faults with displacement less than the full resolution of

* Corresponding author. Fax: +47-55-58-94-16.
E-mail addresses: haakon.fossen@geol.uib.no (H. Fossen), jonhe@statoil.com (J. Hesthammer).

0191-8141/00/$ - see front matter
PII: S0191-8141(00)00013-4

the data can be estimated by extrapolating the straight segment in the log–log plot into the sub-resolution size domain. This is frequently being done and used as input to reservoir modeling in oil fields throughout the world (Childs et al., 1990; Gauthier and Lake, 1993). However, it hinges on the assumption that the scaling law for sub-resolution faults is identical or at least close to that established from the available fault data.

Fracture frequency data from well core studies have here been used to 'test' the reliability of down-scaling below seismic resolution. The limited number of published studies of this kind gives the impression that core data generally fit the predicted small-scale fracture densities (e.g. Walsh et al., 1991; Roberts et al., 1993; Marrett et al., 1999). This correspondence lends support to the reliability of down-scaling of fault displacement populations from the seismic scale to the core scale. Below we present data indicating that this may not always be the right conclusion, potentially leading to serious mistakes if used in strain calculations or oil reservoir management.

2. Geologic setting

The Gullfaks oilfield in the North Sea (Fig. 1) contains abundant seismic and well data from a faulted Late Triassic–Jurassic reservoir section (Fig. 2). Situated in block 34/10 along the western flank of the Viking Graben, the field covers an area of 55 km^2 and occupies the eastern half of the 10–25-km-wide Gullfaks fault block (Fossen et al., 2000). The area has been affected by a Permo-Triassic and a late Jurassic to early Cretaceous rift phase (e.g. Badley et al., 1988; Gabrielsen et al., 1990; Roberts et al., 1995).

The Gullfaks fault block is one of the first-order ~N–S elongated fault blocks in the North Sea rift system. The fault block shows evidence of strong internal deformation, mostly expressed by a domino fault sys-

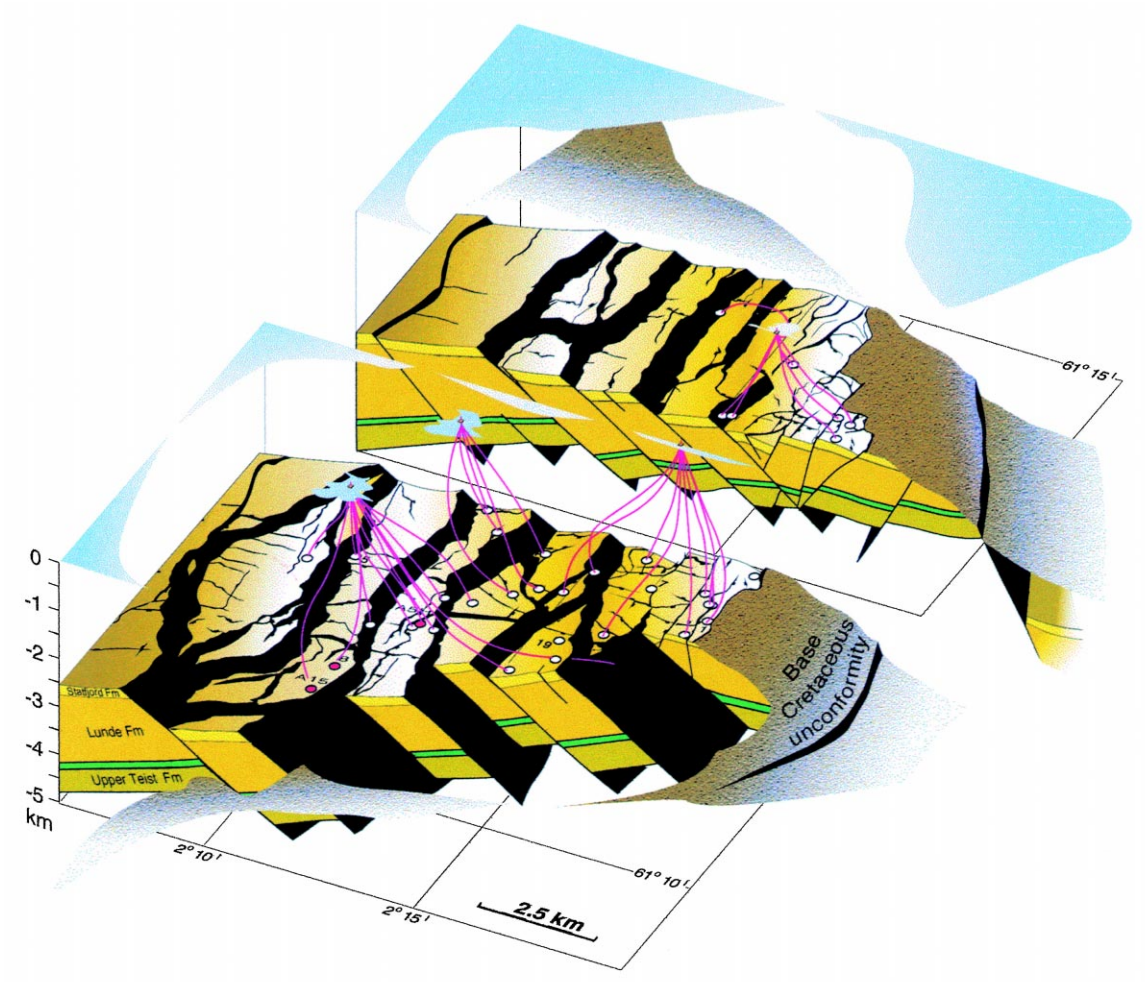

Fig. 1. Geologic perspective of the Statfjord Formation (lower part of the Jurassic reservoir section) of the Gullfaks Field, northern North Sea. Well paths from the three platforms are shown for wells that reach the Statfjord Formation. Note that the number of seismically resolvable faults is higher for overlying formations (not shown) (Fossen and Hesthammer, 1998a).

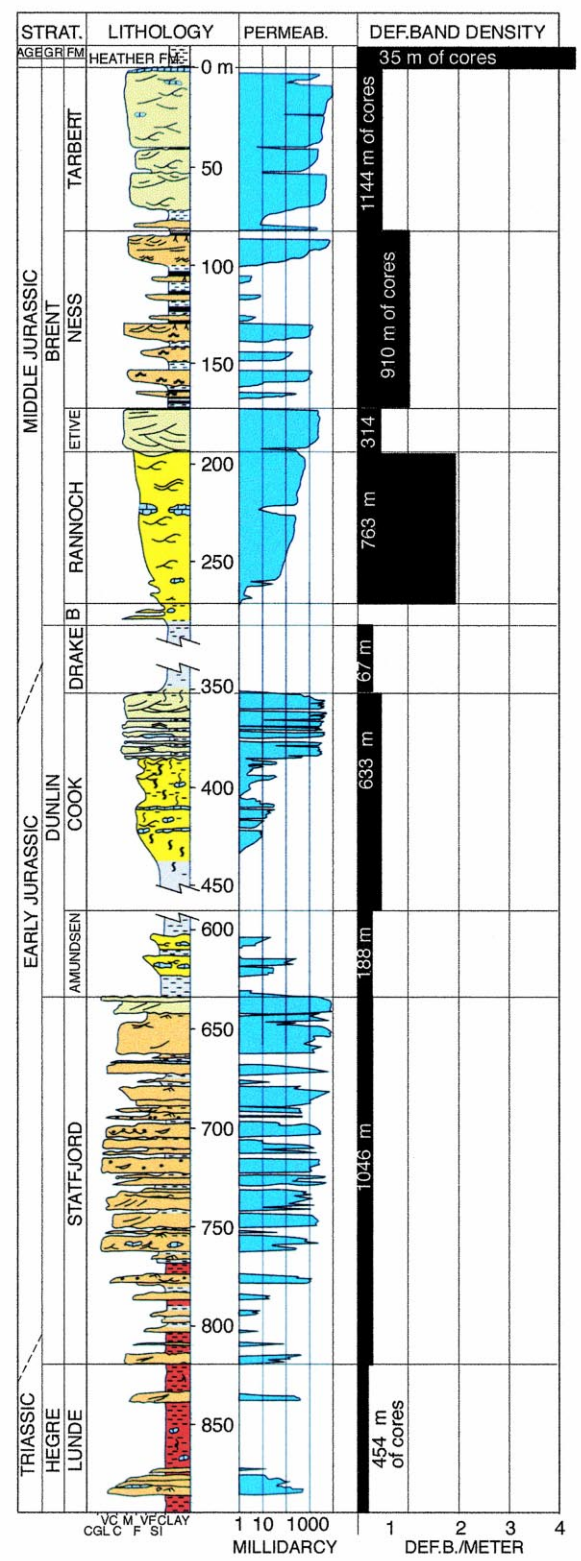

Fig. 2. Stratigraphic column of the cored section of the Gullfaks Field. Average deformation band density is shown for each formation according to the present core study. Also shown is the length (in meters) of the cored interval for each formation. The anomalously high deformation band density for the upper interval (Heather Formation) is based on very limited core information and is not considered to be representative.

tem with east-dipping faults and west-dipping strata. In addition, a deeply eroded horst complex occurs along the eastern margin of the Gullfaks fault block (Fossen and Hesthammer, 1998a).

The drilled stratigraphic section (Fig. 2) starts with continental sandstones, claystones and shales of the Triassic Hegre Group, alluvial sandstones of the Rhaetian–Sinemurian Statfjord Formation, Sinemurian–Toarcian marine clay and siltstones of the Amundsen Formation, regressive, marine, silty claystones, muddy sandstones and sands of the Cook Formation, and marine shales and siltstones of the Drake Formation. The Bajocian–Early Bathonian Brent Group forms the uppermost, and most important, part of the reservoir. The Brent Group comprises deltaic sandstones of the Broom, Rannoch and Etive Formations, interbedded sandstones, shales and coals of the Ness Formation, and excellent reservoir quality sandstones of the uppermost Tarbert Formation. The Brent sandstones have porosities between 20 and 34%, whereas deeper sandstones have somewhat lower porosities.

The reservoir rocks of the Gullfaks Field are capped by Upper Cretaceous shales and siltstones. An unconformity, representing a time gap of up to 100 My, defines the base of the Cretaceous sedimentary rocks. The Cretaceous strata post-date the major part of the faulting history of the Gullfaks Field. Locally, up to 100 m of the Upper Jurassic Heather Formation is preserved in the hanging walls to the main N–S-trending faults.

A total of 130 km of reservoir rocks has so far been penetrated by more than 180 wells on the Gullfaks Field. In addition to standard well-log data (gamma ray, resistivity, neutron/density and sonic velocity logs), 34 km of dipmeter data and more than 6 km of core data were collected for detailed stratigraphic and structural studies. The unusually large amount of information from the field makes it particularly suitable for statistical fault analysis as well as other structural analyses. Below we utilize seismic data, stratigraphic (well-log correlation) data and core data in an attempt to cover a large range in displacement from an extensional fault population.

3. Seismic data

Several three-dimensional seismic surveys have revealed and confirmed the general structure of the Gullfaks area. The dominating domino system is characterized by more or less N-striking faults with displacements up to 500 m. The faults dip 25–30° to the east, whereas bedding has an average dip of 15° to the west, steepening to the east. A several-hundred-meter-wide hanging wall syncline is typically developed along the upper part of these faults.

A number of minor faults with offsets less than 80 m compartmentalize the domino fault blocks and have been related to internal block deformation during differential slippage along the main N-striking faults.

Multiline one-dimensional samples of fault throw from the Early Jurassic top Statfjord Formation seismic interpretation does not conform to a single, well-defined scaling law (Fig. 3) (Fossen and Rørnes, 1996). When compared to the well-log data (see below), it appears that faults with throw less than ~80 m are underrepresented in the seismic interpretation (Fig. 3). Above this size, fault densities match those calculated from stratigraphic well data (see below). These characteristics may be related to the variable quality of the seismic data across the field (Hesthammer and Henden, 2000).

There is also a significant difference in sampling method between the two data sets. Fault throws were sampled from the top Statfjord Formation reflection along evenly spaced E–W-oriented seismic profiles throughout the field, hence undersampling the many minor E–W faults in the field. On the contrary, well data (below) were collected along well paths ranging in inclination from horizontal to vertical and azimuth from 0 to 360°. Furthermore, the well (and core) data were collected from the entire Jurassic stratigraphic sequence, not along a single stratigraphic boundary. The two data sets are thus not directly comparable (also see Fossen and Rørnes, 1996).

4. Stratigraphic well data

Systematic interpretation and correlation of various well-log signatures (gamma ray, neutron, density and resistivity logs) together with core data in the Gullfaks Field has led to detailed knowledge of the local stratigraphy. The high well density gives good control on lateral facies variations, and as a result, thickness anomalies down to 5–10 m can be identified through well-log correlation (Fig. 4). If the anomalies are difficult to explain by sedimentary facies variations, convention among well-log interpreters is that they are attributed to faulting. The success of this method on the Gullfaks Field relies on experienced log interpreters (sedimentologists) who have gained detailed knowledge of the stratigraphy and facies variations through years of well-log interpretation and stratigraphic core studies from the more than 180 wells on the Gullfaks structure.

Plotting the missing section of faults deduced from stratigraphic correlation (Fig. 4) displays a power-law scaling law from ~100 m down to 9 m, i.e. well below full seismic resolution. Missing section (stratigraphic section missing along the well path due to faulting) is identical to throw for horizontal layers. For dipping

layers the deviation depends on the dip of the fault as well as dip of layering. A representative estimate for the Gullfaks reservoir is that missing section exceeds throw by around 15–20%. This relationship may result in some scatter in Fig. 3, but in log–log diagrams the effect is small or negligible. The exponent (D) is found to be 0.6 for the entire data set from the field (128.4 km of drilled reservoir, 277 faults recognized) and 0.67 if only data from the cored section (6.077 km, 18 faults) are considered. By involving this type of data, a throw scaling law, which in the present case was impossible to predict from the seismic data, has been established from ~100 m and well into the gap between seismic and core data. It is important to note that the well-log fault data applied in this work are collected from exactly the same lines through the reservoir as the core data (below), which allows for more reliable and direct comparison.

5. Core data

Structural examination and mapping of all available cores from the Gullfaks Field was performed (Hesthammer, 1999). Care was taken to distinguish tectonic fractures from those formed during drilling or core handling. Abundant bedding-parallel fractures developed due to the pressure release that occurs when the cores are elevated from reservoir levels (at approximately 2 km depth) to the surface. In addition, open fractures subparallel to the borehole resulted from torque during sampling or, less likely, from pressure release in the reservoir. The tectonic fractures typically show evidence of shear displacement, drag or reorientation of layering or platy minerals, disaggregation structures and minor cataclasis, and are in most cases associated with deformation band cluster zones or damage zones around faults. Mineral-filled fractures are rare. Open fractures with no indication of slip were not included in this study.

5.1. Deformation bands

The vast majority of tectonic fractures observed in the cores classify as deformation bands as defined by Aydin and Johnson (1978, 1983), Underhill and Woodcock (1987), Antonellini et al. (1994), Fossen and Hesthammer (1997), and Gabrielsen et al. (1998). These workers describe deformation bands as common constituents of deformed porous sandstones that form mm-thick shear zones with mm- or cm-scale displacement. Two stages or types of deformation bands are

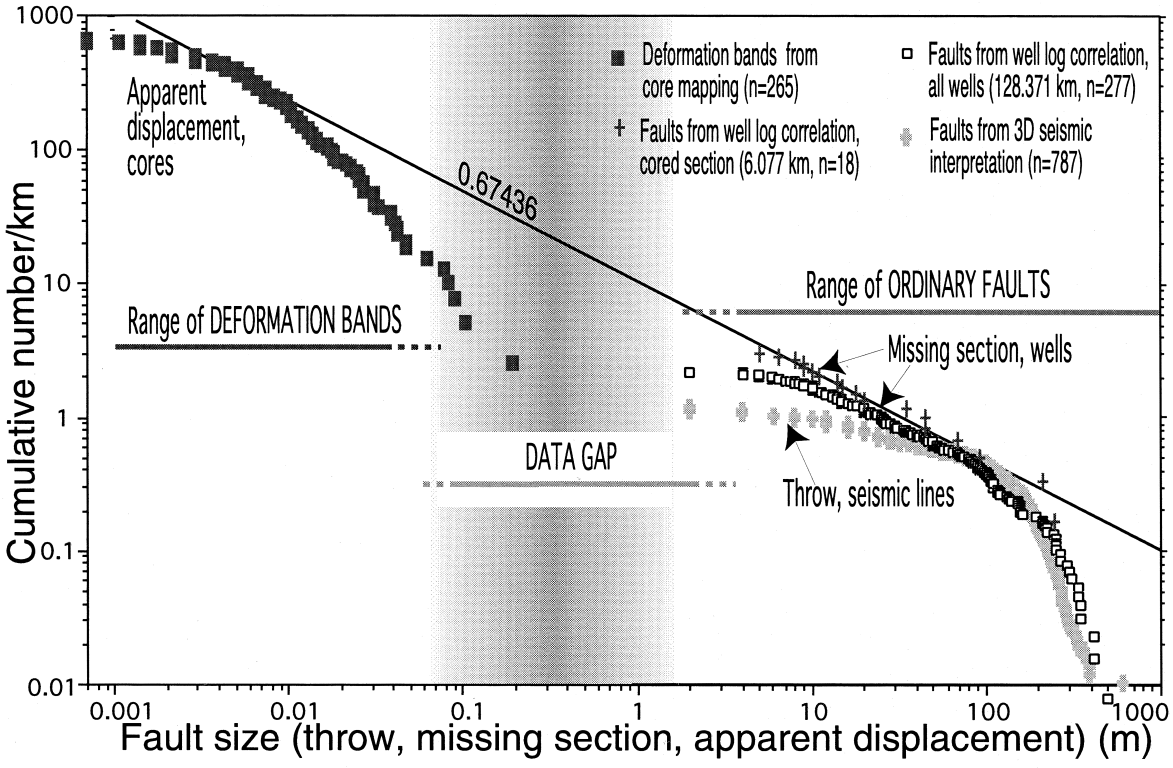

Fig. 3. Cumulative frequency plot of faults and deformation bands from the Gullfaks Field, northern North Sea. Note that faults in the range from 10 cm to 10 m are highly underrepresented. Straight line with slope 0.67 is a linear regression based on missing section data from log correlation from the cored sections. Although throw, missing section and apparent displacement are not directly comparable, the errors are found to be very small in the log–log plot. See text for discussion.

easily discernible; those that only involve reorganization of grains to (generally) denser packing, and those that involve additional and more effective porosity reduction by cataclastic processes. Moreover, deformation bands are generally believed to strain harden during growth. Strain hardening explains why individual bands stop growing after achieving mm- or cm-scale displacement and develop cluster zones rather than discrete fault surfaces.

A total of 4219 deformation bands were mapped in the cored sections from the Gullfaks Field. These deformation bands only rarely show clear evidence of cataclasis. Instead, disaggregation structures dominate the clean sandstones, and phyllosilicate framework structures characterize mica-bearing sandstones. The absence of cataclasis is probably related to the very shallow (up to a few hundred meters; Fossen and Hesthammer, 1998a) burial at the time of deformation. The Gullfaks deformation bands show an average apparent (minimum) dip of about 50° for both E- and W-dipping structures in vertical wells (Hesthammer, 1999), i.e. considerably steeper than the 25–30° dipping domino faults mapped from the seismic data in the area.

Permeability reduction across the deformation bands depends on the amount of phyllosilicates present and is generally negligible in clean sandstones, but increases rapidly with increasing phyllosilicate content. The thickness of the deformation bands increases with grain size in sandstones, from an average of 0.5 mm in very fine-grained sandstones up to 3.5 mm in very coarse-grained lithologies. However, no significant correlation is found between thickness and displacement (Fig. 5) for the deformation bands, contradicting the general presumption of a linear relationship between the two (e.g. Hull, 1988).

As much as 72% of the deformation bands exist within fault damage zones that seldom exceed a few tens of meters in thickness. Also, many of the deformation bands outside of these zones occur together in networks or smaller cluster zones. This occurrence strongly supports the interpretation of these structures as tectonic features.

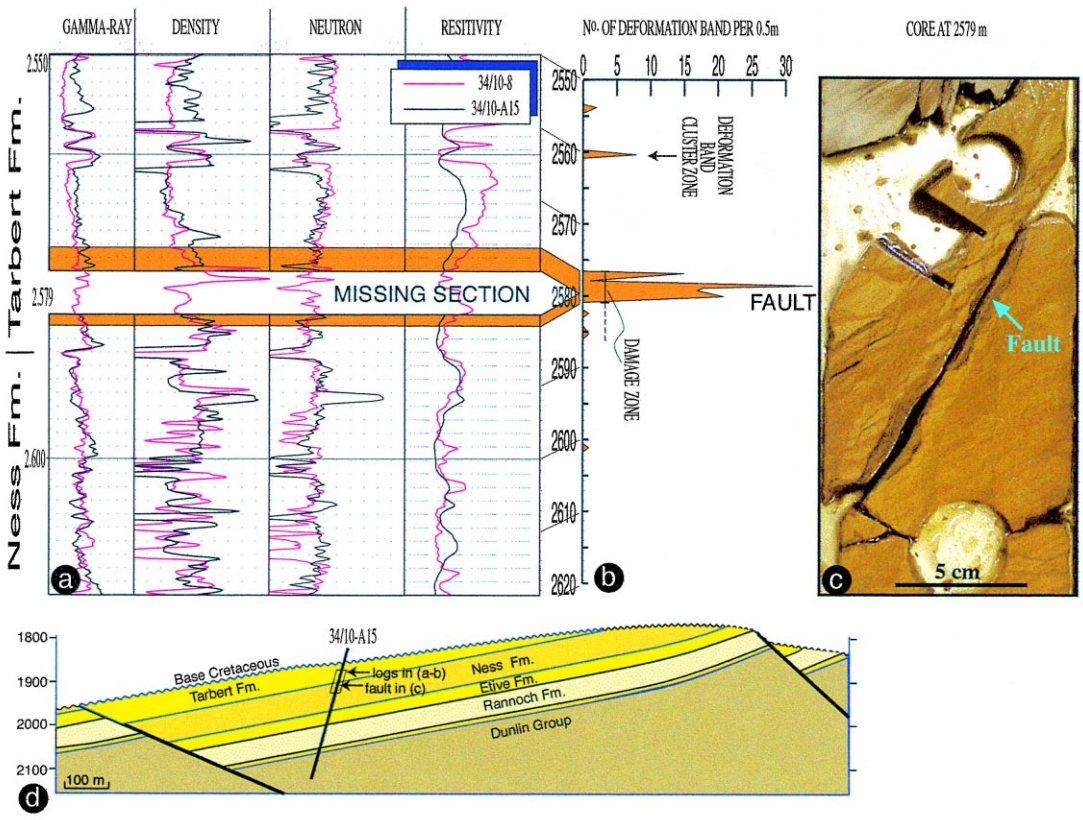

Fig. 4. (a) Example of fault identification through log correlation (measured depth). In the present case (well 34/10-A-15) a 6-m fault has been identified in the basal part of the Tarbert Formation of the Brent Group (Fig. 2). A fracture frequency log (b) from core analysis in the same interval shows the clear relation between deformation band intensity (damage zone) and the fault. Immature fault zones (deformation band cluster zones without fault slip plane) may be present above the fault. The fault was originally picked by sedimentologists at 2580 m. Later core studies showed that the correct position is 2579 m. (c) Photo of the fault at 2579 m. (d) Location of well 34/10-A-15 in one of the domino fault blocks. Location of subseismic fault and log interval are indicated.

5.2. Faults

Faults are distinguished from the deformation bands by their considerably larger displacement along a discrete slip surface. Where observable, the fault surfaces are striated and polished whereas the deformation bands are not. Most of the faults in the cores were already identified by stratigraphic well-log correlation and thus have displacements in excess of ~6 m (the minimum displacement detected by well-log correlation). The identification of faults from log data was arrived at independently but correlates well with the core data once core-log shifts are accounted for. When the position of these 18 faults were checked against the cores, they were typically off from obvious fault location in the cores by a meter or two. This inconsistency confirms that core information was not used during fault location by well-log correlation.

A close association is seen between faults and deformation bands. The sedimentologists suggested a total of 20 faults, identified independently from well-log correlation. Core inspection showed that 18 of these were located within zones of densely clustered deformation bands, which we interpret as damage zones. The others were two 6-m faults suggested in wells 34/10-A-5H and A-8. The 34/10-A-8 section is covered by continuous cores that show little or no indication of either faults or deformation bands. This stratigraphic anomaly has therefore been reinterpreted as primary facies variations. The 34/10-A-5H anomaly is not completely

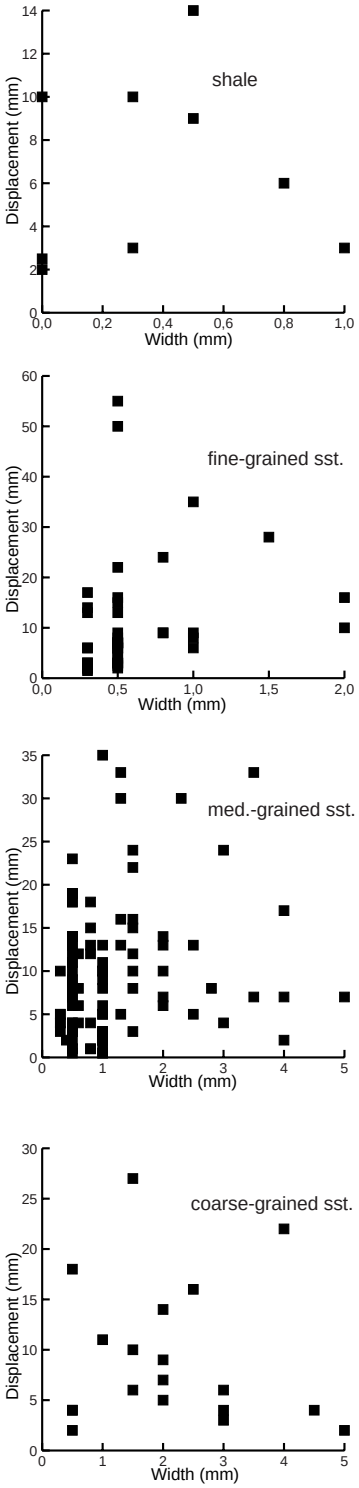

Fig. 5. Displacement–thickness data for deformation bands, separated with respect to grain size of the host rock. See text for discussion.

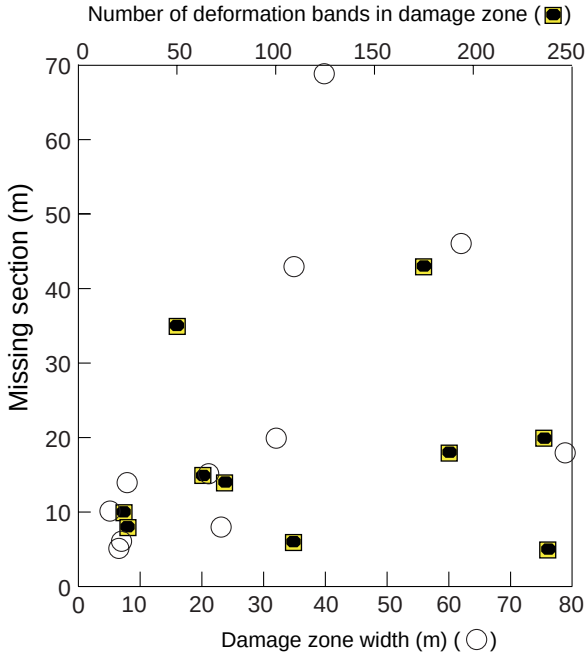

Fig. 6. Diagram showing the number of deformation bands contained in known fault damage zones in the Gullfaks cores (filled circles) and the thickness of the damage zone (open symbols) with respect to missing section. The thinnest damage zone is 5 m and contains 23 deformation bands. The numbers are minimum estimates, as the closely spaced deformation bands may be difficult to separate. The widest damage zone observed is a 35 m fault with >150-m-wide damage zone that falls outside this graph.

cored, but is likely to be another example of facies variation. All of the 18 faults have damage zones containing 23 or more deformation bands, and damage zone thickness fall in the range of 5–150 m (Fig. 6).

In addition to the 18 faults identified from well-log correlation, a number of deformation band cluster zones are mapped in the cores. Only three of these zones exhibit thickness and deformation band frequencies comparable to fault-related damage zones (≥23 deformation bands within a ≥5-m-wide zone; see Fig. 6). Although evidence of discrete faulting was not observed, these three deformation band zones may indicate fault locations. The rest of the cluster zones are narrower and contain fewer deformation bands than damage zones to the 18 faults. Twelve of these narrower zones contain 23 deformation bands or more (i.e. comparable to the known 18 faults), 17 contain fewer than 23 but more than five deformation bands, and about 40 consist of 2–5 deformation bands (data presented in Hesthammer, 1999). These cluster zones may be forerunners to mature fault structures (see below), and some may contain faults below the resolution of well-log correlation (Fig. 4). In the latter case, their slip (fault) surfaces must be hidden in drilling-induced rubble zones or small sections removed for sampling (seal peals), but where cores are completely continuous through these residual cluster zones (four cases), such slip surfaces have not been observed.

5.3. Displacement

Measurable apparent displacement on 265 deformation bands in the cores averages about 8 mm. Most deformation bands occur in cluster zones or lack characteristic offset markers, which makes observation of displacement impossible. The collected displacement data are plotted together with throw (and missing section) data in Fig. 3. Since displacement values exceed throw by an amount depending on the dip of the deformation bands, the data sets are not directly comparable. Apparent dips of deformation bands in the cores average around 50°. Based on the simplifying assumption that true dip of the deformation bands is at least 50° (implying that throw is less than displacement by an average factor >0.8), a throw population was calculated and plotted for comparison, but the difference was almost invisible in log–log space.

The fact that apparent rather than true displacement is measured is another source of error. The true displacement data would plot somewhat to the left of the apparent displacement points in Fig. 3 by an amount depending on the angle between the deformation band and the core section, and therefore differs for each data point. This non-linear relation also affects the shape of the curve outlined by the displacement data. Again, the visual effect in a log–log plot would not be great, nor critical for comparison with well log and seismic data.

The deformation band data do not define a straight line segment in Fig. 3, a feature possibly influenced by the likely undersampling of 'large' (>1 cm) displacements in cores. However, the low end of the data plots remarkably close to the straight line calculated for the larger faults determined from well-log correlation from the cored section ($D = 0.67$), separated by a data gap between 0.2 and 6.5 m. It is thus tempting to suggest that the entire fault population with displacement from the mm to 100 m scale obeys this scaling law, and that the data gap is a result of incomplete data collection, as suggested in several previous studies (e.g. Needham et al., 1996; see, however, Koestler, 1994). Below we will discuss why we suspect that this may not be the case in the Gullfaks reservoir sandstones.

6. Discussion

6.1. How many unidentified faults would it take to fill the gap?

A data gap exists between the largest displacements seen in cores (~20 cm) and the smallest displacements seen from stratigraphic well-log correlation of the cored section (6.5 m). Extrapolation of the scaling law established for large faults down to deformation bands predicts 31 faults/km with displacement in the range 20 cm–6.5 m, i.e. 169 faults that were not observed in the cored section. Evaluation of fault displacements in this size range is generally considered to be difficult for sub-surface oil reservoir rocks. We will here use the observation that damage zones are associated with the Gullfaks faults to approach this problem.

6.2. How many faults may be available?

In the present case the 18 faults seen from well-log correlation are easily identified in the cores by their characteristic damage zones (deformation band cluster zones). This important finding strongly suggests that *all faults in the study area exhibit damage zones, and hence can easily be recognized in the cores*. In other words, single slip surfaces may be hidden throughout the cored section, whereas the much thicker damage zones are easily detected.

As argued above, only three additional cluster zones of similar thickness are found (Hesthammer, 1999). Likewise, only 12 additional cluster zones with comparable number of deformation bands occur. If these cluster zones indicate faults, their displacement is expected to be less than 6.5–9 m (resolution of well-log data). Deformation band cluster zones with between 22 and six deformation bands amount to 17. Hence, if

all deformation band cluster zones with more than five deformation bands are considered to contain faults, which seems unlikely, the maximum number of faults with throw greater than that of single deformation bands but less than the faults detected from well-log correlation is, from these considerations, 3 + 12 + 17 = 32.

Several small core intervals are intensely fractured and present as rubble zones or, less commonly, simply lack cohesion (sand intervals). It is well known that such zones form during drilling operations, and the intervals may potentially hide fault structures and/or deformation bands. Except for the relatively few non-cohesive sand intervals, rubble zones contain fragments that were carefully examined for tectonic structures. Deformation bands were easily detected in minor rubble zones in damage zones to the 18 known faults. One would therefore expect to see deformation bands in other rubble zones at locations of tectonic deformation. Deformation structures of possible or likely tectonic origin were recorded from about 60 of the rubble zones, but none of these zones come close to the 5-m thickness of the damage zones associated with the 18 known faults (the widest zone is 1.66 m). None or very few of these rubble zones are therefore considered to hide faults.

There are minor intervals that have not been cored between the starting and ending point of the cored sections in each well. These intervals, which are additional to the 6.077 km cored section, vary greatly in size, and their presence may have several explanations. In many cases they are predetermined by the coring program, in other cases cores are missing due to technical difficulties during drilling operations. Some 25 of these missing core intervals are 5 m wide or more, and thus reach the thickness of fault damage zones. Fault/damage zone structures may be located to some of these 25 intervals. The possibility that rubble zones form more easily at fault locations than elsewhere should be kept in mind. However, the fact that none of the 18 faults observed from well-log correlation are represented as rubble zones (except for very limited intervals) suggests that there is no significant correlation between fault location and coring problems. Thus, considering the fault density of about 30 per km calculated above, one would expect only a few, if any, faults at these locations.

The largest recorded (apparent) slip along a deformation band is on the order of 20 cm. Given the restricted core diameters, larger displacements may exist in the drilled section. Displacement was only detectable from a small portion of the deformation bands (6.3%). This small percentage is mostly explained by the clustering nature of deformation bands. About 80% of the deformation bands occur in cluster zones, in which displacement on individual

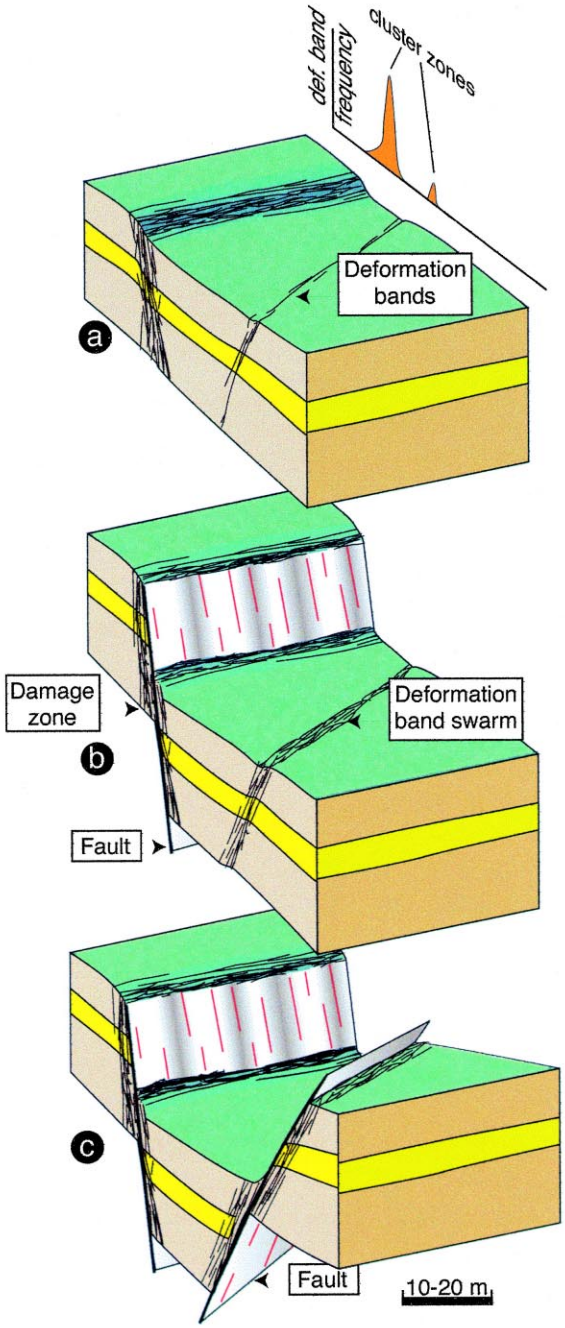

Fig. 7. A simple model for fault development, originally used to explain data from Jurassic sandstones in Utah (Aydin and Johnson, 1978). Deformation bands grow in number due to strain hardening, and link to form swarms or cluster zones. At some point, a fault breaks through the zone, leaving the deformation band swarm as a passive damage zone around the fault. Linking of the fault with other faults of similar or greater size may cause an underrepresentation of small fault displacements larger than those of deformation bands.

bands generally is unknown. For the remaining 14%, displacement is at least partly hidden due to lack of characteristic markers, but in some cases displacements may be larger than the cored lengths of the deformation bands. Unfortunately, since no significant relationship between deformation band thickness and displacement seems to exist (Fig. 5), thickness data cannot be used to infer displacement. On the other hand, general knowledge of displacement associated with deformation bands indicates that they seldom exceed some centimeters or a few tens of centimeters (e.g. Aydin and Johnson, 1978; Antonellini et al., 1994; Lothe, 1998).

In order to fill the gap completely, we need all of the 15 additional deformation band cluster zones with band population similar to the 18 known faults, the 17 smaller cluster zones with between 23 and six deformation bands, and the fault locations at each of the 60 rubble zones that contain signs of deformation structures as faults. Additionally, we need to infer that 77 deformation bands have considerably larger displacements than those observed in the cores and/or that clusters of five or fewer deformation bands mark fault locations. Based on our experience from core evaluation and the field, we find this scenario to be unlikely.

6.3. Damage zone thickness–fault size relationship

As indicated above, the known faults in the cored section exhibit damage zones with a minimum of 23 deformation bands and 5 m of thickness, and hence can easily be identified in the cores. If smaller faults have narrower damage zones, then they would be more difficult to identify. Knowledge of how the damage zones vary in size with respect to fault displacement is thus of major importance in this context.

There are several factors that may contribute to the formation and growth of damage zones. It is clear that deformation bands in many, if not all, cases form prior to the formation of a distinct slip surface (fault). A simple model, which has strong support in deformed porous sandstones, is the one where short-lived deformation bands grow in number to form a cluster zone, which at some point is accompanied by a slip (fault) surface (e.g. Aydin and Johnson, 1983; Underhill and Woodcock, 1987; Fossen and Hesthammer, 1998b) (Fig. 7). This development has recently been observed in physical experiments (Mair et al., 2000). The rapid death (small displacements) of individual deformation bands is traditionally related to strain hardening as grains interlock and the rock compacts, although strain hardening is not a necessity (Harper and Lundin, 1997). The damage zone becomes frozen in as the weak slip surface forms, and the characteristic thickness of the damage zone probably depends on lithological (rheological) properties and confining pressure. As the slip surface grows, deformation bands probably form in the process zone ahead of the slip surface tip line (e.g. Scholz et al., 1993).

The damage zone growth may recur due to increasing wall rock strain during slip accumulation along the slip surface. Also, the slip surface may lock or become resistant against continued slip due to geometrical complications along non-planar fault surfaces, as the fault tip meets new lithologies, during fault linkage, or due to interference with other deformation band zones or fault structures. The total effect would be a somewhat unpredictable scatter in fault displacement–damage zone thickness diagrams, although with a positive correlation between displacement and thickness.

As expected from the above discussion, the Gullfaks damage zone thickness–displacement data (Fig. 6) show a large scatter, although with a positive correlation. It may be noted that several (1/3) of the damage zones have thickness values in the range 5–8 m. Although the amount of data is limited, this grouping may possibly indicate the initial size of damage zones during slip surface formation. This suggestion is supported by the fact that no fault (slip) surface is observed in or near narrower cluster zones in the cored section.

The alternative view is that slip surfaces form at an earlier stage, say with an initial damage zone thickness of one meter or, less likely, that damage zones grow along with displacement from the scale of individual deformation bands. In this scenario, damage zones become narrower for smaller fault sizes also within the (upper part of the) data gap. Plotting the damage zone information from the Gullfaks study in log–log space (Fig. 8) emphasizes the positive correlation between displacement and damage zone thickness. Deformation band data have also been included for comparison in this figure, as done in previous studies (e.g. Knott et al., 1996), although one should be aware that the process involved during deformation band growth and damage zone growth are not directly related. With this important fact in mind, a regression line can, in lack of other, more appropriate data, be fitted to the combined deformation band and fault data. The calculated trend in Fig. 8, together with the trend shown in Fig. 3 predicts 35 faults in the data gap with damage zones equal to or larger than 1 m.

From the core study we found 18 cluster zones $\geq$1 m thick that were not regarded as faults by the sedimentologists during log correlation. These zones may account for some of the 35 faults, although the absence of slip surfaces associated with these zones argues against such an interpretation. At least three of these cluster zones appear related to faults outside the cored interval. Only seven of the rubble zones with deformation structures have intervals of 1 m or more. Other faults with $\geq$1-m-wide damage zones do not

appear to exist in the cored section, unless they are hidden in rubble zones in which we have failed to find deformation structures. It is thus possible to explain the data gap in this way, but perhaps not very likely.

As indicated above, there is no obvious reason why deformation bands should fall on the extrapolated trend of the displacement–thickness relationship for faults with slip surfaces. Other studies indicate that damage zone thickness–displacement confirm to a linear relationship if considered over a large enough range in data (Scholz, 1987; Hull, 1988; Knott et al., 1996), although variations are expected (Evans, 1990). Adopting this view, and considering the dashed line ($D = T$) with slope = 1 that goes through the fault data in Fig. 8, predicts 45 rather than 35 unseen faults with damage zones thicker than 1 m.

6.4. Possible explanations for the data gap

A relevant question is how to treat the deformation band cluster zones without slip surfaces. If each of these zones is considered to be a fault structure with its cumulative displacement as the fault displacement, the gap may more easily be filled. However, these same deformation bands would also have to be included in the low end of the curve to obtain the fit between the well-log correlation/seismic data and the core data. Using the same displacement data twice is probably not a reasonable way of treating the data in this context.

One possible explanation for a data gap may be the close spacing of faults in the Gullfaks Field. The high fault density caused most faults to coalesce during growth. For the same reason a displacement–length relation is not possible to establish for the faults in the Gullfaks Field, but general knowledge indicates that faults with displacement around 5 m tend to have lengths of the order of 1 km. The distance to the nearest fault from any given point in the field is likely to be considerably smaller than this (Fig. 1). The result is that the low-displacement portion of fault surfaces is missing for most faults, and thus underrepresented. At the same time, deformation bands only seldom develop displacements much in excess of ~10 cm, thus forming a low-displacement population, which, by coincidence, falls close to the extrapolated trend of the Gullfaks well data.

Finally, data gaps have been reported from western Sinai that may be related to lithological variations or mechanical stratification (Koestler, 1994; Knott et al., 1996). Furthermore, Wojtal (1994) pointed out that faults and fault displacements can be very differently distributed in neighboring layers, each with different scaling laws. Of particular relevance is a data gap in the Sinai data for throws around 5 m, which was related to the thickness of the lower, sandy part of the ~300 m thick Nubian sandstone (Knott et al., 1996). However, the extreme mechanical contrast between the Nubian sandstone and the underlying basement (and overlying limestone) has no counterpart in the Gullfaks reservoir. The distribution of deformation bands in the Gullfaks Field (Fig. 2) appears to be higher for the ~150 m of sand-dominated Rannoch–Ness formations. Whether this finding is significant and related to the data gap cannot be evaluated properly without much more structural information from the reservoir.

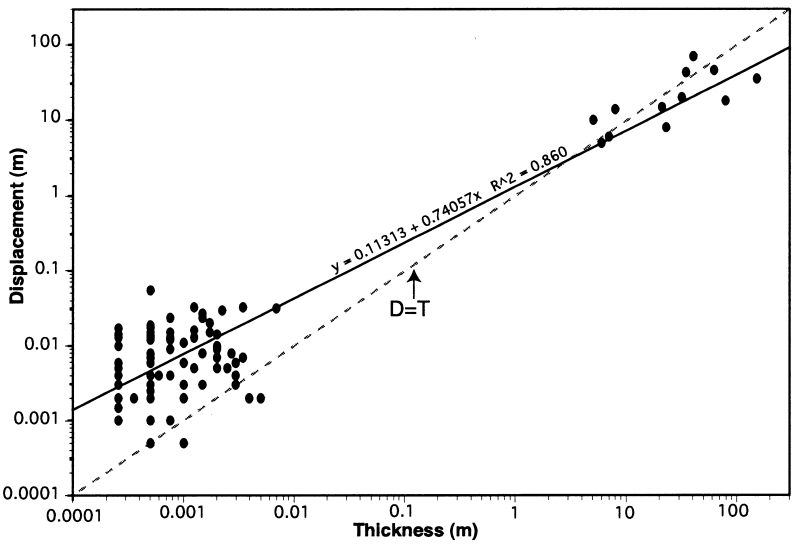

Fig. 8. Displacement–thickness data for deformation bands and faults plotted together in log–log space. A slope is calculated for the combined data set. A linear relation between D and T is indicated for reference, where $D = T$.

7. Conclusions

Fault displacements, as determined from well-log correlation in the cored section of the Gullfaks Field reservoir in the North Sea define a scaling law which, if extended from 6.5–150 m into the mm–cm scale size range, fits the deformation band data extracted from the cores. The deformation bands tend to cluster around known faults in the Gullfaks Field to form damage zones, revealing their tectonic nature. All known faults in the 6.077 km cored section exhibit damage zones that are 5 m wide or more, consisting of at least 23 deformation bands. The data gap that exists between 0.1 and 6.5 m is difficult to fill if all faults have damage zones with more than five deformation bands. We therefore suspect that the data gap may, to some extent, be real. The high fault density in the field, and/or influences of mechanical layering may have caused the data gap.

Although more data need to be collected and analyzed from other locations to test the generality of the observations made in this contribution, under-representation of faults with throw between ~10 cm and ~5 m in some faulted, porous sandstones means that downscaling of faults from seismic to the subseismic size domain may lead to erroneous reservoir descriptions. Even in cases where available structural core data fit the microfault density predicted by the downscaling, one should consider the possibility that the intermediate size-range may be missing.

Acknowledgements

We thank the Norwegian oil companies Statoil and Norsk Hydro for permission to publish this work. The contents of this paper benefited significantly through careful reviews by Tim Needham and John Walsh, and from editorial comments by Jim Evans.

References

Antonellini, M.A., Aydin, A., Pollard, D.D., 1994. Microstructure of deformation bands in porous sandstones at Arches National Park, Utah. Journal of Structural Geology 16, 941–959.

Aydin, A., Johnson, A.M., 1978. Development of faults as zones of deformation bands and as slip surfaces in sandstones. Pure and Applied Geophysics 116, 931–942.

Aydin, A., Johnson, A.M., 1983. Analysis of faulting in porous sandstones. Journal of Structural Geology 5, 19–31.

Badley, M.E., Price, J.D., Dahl, C.R., Agdestein, T., 1988. The structural evolution of the northern Viking Graben and its bearing upon extensional modes of basin formation. Journal of the Geological Society, London 145, 455–472.

Childs, C., Walsh, J.J., Watterson, J., 1990. A method for estimation of the density of fault displacements below the limits of seismic resolution in reservoir formations. In: Graham, Trotman (Eds.), North Sea Oil and Gas Reservoirs—II. The Norwegian Institute of Technology, pp. 309–318.

Evans, J.P., 1990. Thickness–displacement relationships for fault zones. Journal of Structural Geology 12, 1061–1065.

Fossen, H., Hesthammer, J., 1997. Geometric analysis and scaling relations of deformation bands in porous sandstone. Journal of Structural Geology 19, 1479–1493.

Fossen, H., Hesthammer, J., 1998a. Structural geology of the Gullfaks Field, northern North Sea. In: Coward, M.P., Johnson, H., Daltaban, T.S. (Eds.), Structural geology in reservoir characterization. Geological Society Special Publication, 127, pp. 231–261.

Fossen, H., Hesthammer, J., 1998b. Deformation bands and their significance in porous sandstone reservoirs. First Break 16, 21–25.

Fossen, H., Odinsen, T., Færseth, R.B., Gabrielsen, R.H., 2000. Detachments and low-angle faults in the northern North Sea rift system. In: Nøttvedt, A., Gabrielsen, R., Larsen, T.B. (Eds.), Dynamics of the Norwegian margins. Geological Society Special Publication, 167, pp. 105–131.

Fossen, H., Rørnes, A., 1996. Properties of fault populations in the Gullfaks Field, northern North Sea. Journal of Structural Geology 18, 179–190.

Gabrielsen, R.H., Aarland, R., Alsaker, E., 1998. Identification and spatial distribution of fractures in porous, siliclastic sediments. In: Coward, M.P., Johnson, H., Daltaban, T.S. (Eds.), Structural geology in reservoir characterization. Geological Society Special Publication, 127, pp. 49–64.

Gabrielsen, R.H., Færseth, R.B., Steel, R.J., Idil, S., Kløvjan, O.S., 1990. Architectural styles of basin fill in the northern Viking Graben. In: Blundell, D.J., Gibbs, A.D. (Eds.), Tectonic evolution of the North Sea rifts. Clarendon Press, Oxford, pp. 158–183.

Gauthier, B.D.M., Lake, S.D., 1993. Probabilistic modeling of faults below the limit of seismic resolution in Pelican Field, North Sea, offshore United Kingdom. American Association of Petroleum Geologists Bulletin 77, 761–777.

Harper, T.R., Lundin, E.R., 1997. Fault seal analysis: reducing our dependence on empiricism. In: Möller-Pedersen, P., Koestler, A.G. (Eds.), Hydrocarbon seals—importance for exploration and production. NPF Special Publication, 7. Elsevier, pp. 149–165.

Hesthammer, J. 1999. Analysis of fault geometry and internal fault block deformation in the Gullfaks region, northern North Sea. Dr. scient. Thesis. University of Bergen.

Hesthammer, J., Henden, J., 2000. Closing the gap between theory and practice in seismic interpretation of small-scale faults. Petroleum Geoscience 6, in press.

Hull, J., 1988. Thickness–displacement relationships for deformation zones. Journal of Structural Geology 4, 431–435.

Jackson, P., Sanderson, D.J., 1993. Scaling of fault displacements from the Badajoz–Cordoba shear zone, SW Spain. Tectonophysics 210, 179–190.

King, G., Cisternas, A., 1991. Do little things matter? Nature 351, 350.

Knott, S.D., Beach, A., Brockbank, P.J., Brown, J.L., McCallum, J.E., Welbon, A.I., 1996. Spatial and mechanical controls on normal fault populations. Journal of Structural Geology 18, 359–372.

Koestler, A.G., 1994. Scaling properties of extensional fault populations—the natural gap at the medium scale. Extended abstract: Fault Populations Meeting, Tectonic Studies Group.

Lothe, A.E., 1998. Den strukturelle utviklingen av Brumunddalsandsteinen: forkastningsgeometrier, tilpasningsstrukturer og deformasjonsbånd. Cand. scient. thesis, University of Bergen.

Mair, K., Main, I., Elphick, S., 2000. Sequential growth of deformation bands in the laboratory. Journal of Structural Geology 22, 25–42.

Marrett, R., Allmendinger, R.W., 1992. Amount of extension on "small" faults: an example from the Viking Graben. Geology 20, 47–50.

Marrett, R., Orthega, O.J., Kelsey, C.M., 1999. Extent of power-law scaling for natural fractures in rock. Geology 27, 799–802.

Needham, T., Yielding, T., Fox, R., 1996. Fault population description and prediction using examples from offshore U.K. Journal of Structural Geology 18, 155–167.

Roberts, A.M., Yielding, G., Kusznir, N.J., Walker, I.M., Dorn-Lopez, D., 1993. Mesozoic extension in the North Sea: constraints from flexural backstripping, forward modelling and fault populations. In: Parker, J.R. (Ed.), Petroleum geology of northern Europe. Journal of the Geological Society, London, pp. 1123–1136.

Roberts, A.M., Yielding, G., Kusznir, N.J., Walker, I.M., Dorn-Lopez, D., 1995. Quantitative analysis of Triassic extension in the northern Viking Graben. Journal of the Geological Society, London 152, 15–26.

Scholz, C.H., 1987. Wear and gouge formation in brittle faulting. Geology 15, 495–497.

Scholz, C.H., Dawers, N.H., Yu, J.Z., Anders, M.H., 1993. Fault growth and fault scaling laws: preliminary results. Journal of Geophysical Research 98 (21), 951–961.

Walsh, J., Watterson, J., Yielding, G., 1991. The importance of small-scale faulting in regional extension. Nature 351, 391–393.

Wojtal, S.F., 1994. Fault scaling laws and the temporal evolution of fault systems. Journal of Structural Geology 16, 603–612.

Yielding, G., Walsh, J., Watterson, J., 1992. The prediction of small-scale faulting in reservoirs. First Break 10, 449–460.

Underhill, J.R., Woodcock, N.H., 1987. Faulting mechanisms in high-porosity sandstones: New Red Sandstone, Arran, Scotland. In: Jones, M.E., Preston, R.M.F. (Eds.), Deformation of sediments and sedimentary rocks. Geological Society Special Publication, 29, pp. 91–105.